Available online at www.sciencedirect.com
SCIENCE DIRECT®
Journal of Molecular Spectroscopy 237 (2006) 149–162
Journal of MOLECULAR SPECTROSCOPY
www.elsevier.com/locate/jms

High-resolution Fourier-transform spectroscopy of ^{18}O-enriched water molecule in the 1080–7800 cm^{-1} region

An-Wen Liu, Jun-He Du, Ke-Feng Song, Le Wang, Lei Wan, Shui-Ming Hu *

Hefei National Laboratory for Physical Sciences at Microscale, University of Science and Technology of China, Hefei 230026, China
Shanghai Institute for Advanced Studies, University of Science and Technology of China, Shanghai 201315, China

Received 24 February 2006; in revised form 10 March 2006
Available online 28 March 2006

Abstract

Fourier-transform absorption spectrum of ^{18}O enriched water sample was recorded in the 1080–7800 cm^{-1} region. The transitions of $H_2{}^{18}O$ were assigned on the base of the high accuracy ab initio calculations by Partridge and Schwenke (PS). One thousand two hundred and forty-six ro-vibrational energy levels were retrieved, which belong to the $v_1 + \frac{1}{2}v_2 + v_3 = 0.5$, 1, and 1.5 polyads: (0 1 0), (1 0 0), (0 2 0), (0 0 1), (1 1 0), (0 1 1), and (0 3 0) states. Four hundred and thirty-two of them are reported for the first time. The results are also investigated comparing with the PS calculations and the available literature data in the considered spectral range. $HD^{18}O$ as a small concentration in the sample, more than 4900 transitions were also observed. These transitions yield 1066 ro-vibrational energies of nine vibrational states, 504 energy levels were obtained for the first time.

Keywords: Vibration–rotation spectroscopy; Water vapor absorption; Spectroscopic parameters

1. Introduction

As the second primary isotope of the water molecule, $H_2{}^{18}O$ and its infrared absorption contributes noticeably to the atmospheric absorption and might be taken into account in the explanation of atmospheric radiation balance. In the last few decades, numerous spectroscopic studies on the $H_2{}^{18}O$ molecule have been carried out with microwave [1–5], Fourier-transform infrared [6–24], and cavity ring-down spectroscopy [25,26] in the near-IR and visible region. More than 800 energy levels have been reported from our previous Fourier-transform study [27,28]. All these results including $H_2{}^{18}O$ energy levels, transition frequencies, and strengths are available in the most complete database to date [29]. Despite of all the above undertakings, the high resolution study of $H_2{}^{18}O$ below 1 μm region is not yet complete, compared with the detailed simulation given by Partridge and Schwenke (PS) [30,31]. Many lines predicted with relatively strong and middle intensities are not yet observed. For the $HD^{18}O$ molecule, to the best of our knowledge, only a few bands including ν_1, ν_2, $2\nu_2$, ν_3, $3\nu_2$, and $\nu_1 + \nu_2$[1] have been studied [32–34].

The purpose of this work is, besides of a continuation to our previous studies of the high resolution Fourier-transform absorption spectroscopy of $H_2{}^{18}O$ [27,28], the study of $HD^{18}O$ in the region between 1080 and 7800 cm^{-1} will be also presented. The experimental details, transition assignments, and analysis will be given in the following sections.

2. Experimental details

The ^{18}O enriched water sample was purchased from Aldrich Chemical Company, Inc. The stated isotopic concentration of the ^{18}O atom is 95%. The absorption

* Corresponding author. Fax: +86 551 3602969.
E-mail address: smhu@ustc.edu.cn (S.-M. Hu).

[1] ν_1 and ν_3 present the OD and OH stretching modes of HDO, respectively. ν_2 is for the bending mode.

0022-2852/$ - see front matter © 2006 Elsevier Inc. All rights reserved.
doi:10.1016/j.jms.2006.03.008

spectra were recorded at room temperature with a Bruker IFS 120HR Fourier-transform spectrometer equipped with a path length adjustable multi-pass gas cell. Because of the wide spectral range and the large variation of the absorption line intensities, different experimental conditions were used in the measurements as listed in Table 1. The pressure was measured using two capacitance manometers of 200 Pa and 133 hPa full-scale range with an overall accuracy of 0.5%. In most measurements, optical filters were applied to increase the signal–noise-ratio and to allow the high spectral resolution measurements. The line positions were calibrated with water lines given by the HITRAN2004 [29] database. The accuracy of the line positions of unblended and not-very-weak lines was estimated to be better than 0.0012 cm^{-1}. Parts of two spectrum together with the assignments are presented in Figs. 1 and 2.

Because we could not substitute all the water adsorbed on the walls of the sample cell with the very limited amount of sample, it is difficult to accurately

Table 1
Experimental conditions in the Fourier-transform measurements of ^{18}O enriched water sample

Region (cm^{-1})	Source	Beam splitter	Detector	Path length (m)	Pressure (Pa)	Resolution (cm^{-1})
950–1350	Globar	KBr	MCT	15	1307	0.005
1200–1700	Globar	KBr	MCT	15	126	0.005
1200–1700	Globar	KBr	MCT	15	1307	0.005
800–5000	Globar	KBr	MCT	15	1307	0.008
2500–3350	Tungsten	CaF_2	InSb	15	126	0.005
2500–3350	Tungsten	CaF_2	InSb	15	1307	0.005
2500–3350	Tungsten	CaF_2	InSb	105	1307	0.008
3200–4300	Tungsten	CaF_2	InSb	15	126	0.008
3200–4300	Tungsten	CaF_2	InSb	15	1307	0.008
3900–5100	Tungsten	CaF_2	InSb	105	1307	0.01
4900–6400	Tungsten	CaF_2	InSb	15	11	0.01
4900–6400	Tungsten	CaF_2	InSb	15	126	0.01
4900–6400	Tungsten	CaF_2	InSb	15	1307	0.01
4900–6400	Tungsten	CaF_2	InSb	105	1307	0.01
5000–11 000	Tungsten	CaF_2	Ge	15	215	0.015
5000–11 000	Tungsten	CaF_2	Ge	15	1307	0.015
5000–11 000	Tungsten	CaF_2	Ge	105	1307	0.015

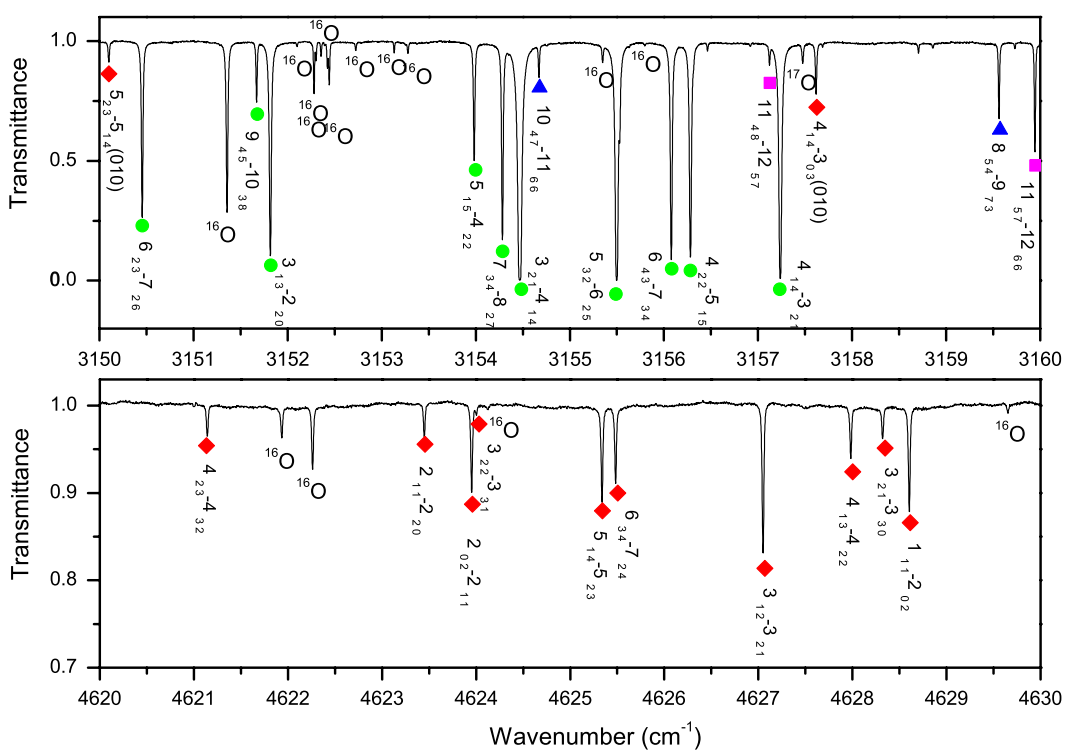

Fig. 1. A small part of the $H_2{}^{18}O$ spectrum and the line assignments of ν_1, ν_3, $2\nu_2$, and $3\nu_2$ bands marked by square, triangle, circle, and diamond, respectively. Experimental conditions: absorption path length 105 m, sample pressure 1307 Pa, unapodized resolution 0.008 cm^{-1}, and 0.01 cm^{-1} for upper and lower panels, respectively. Lines marked with ^{16}O and ^{17}O are due to $H_2{}^{16}O$ and $H_2{}^{17}O$.

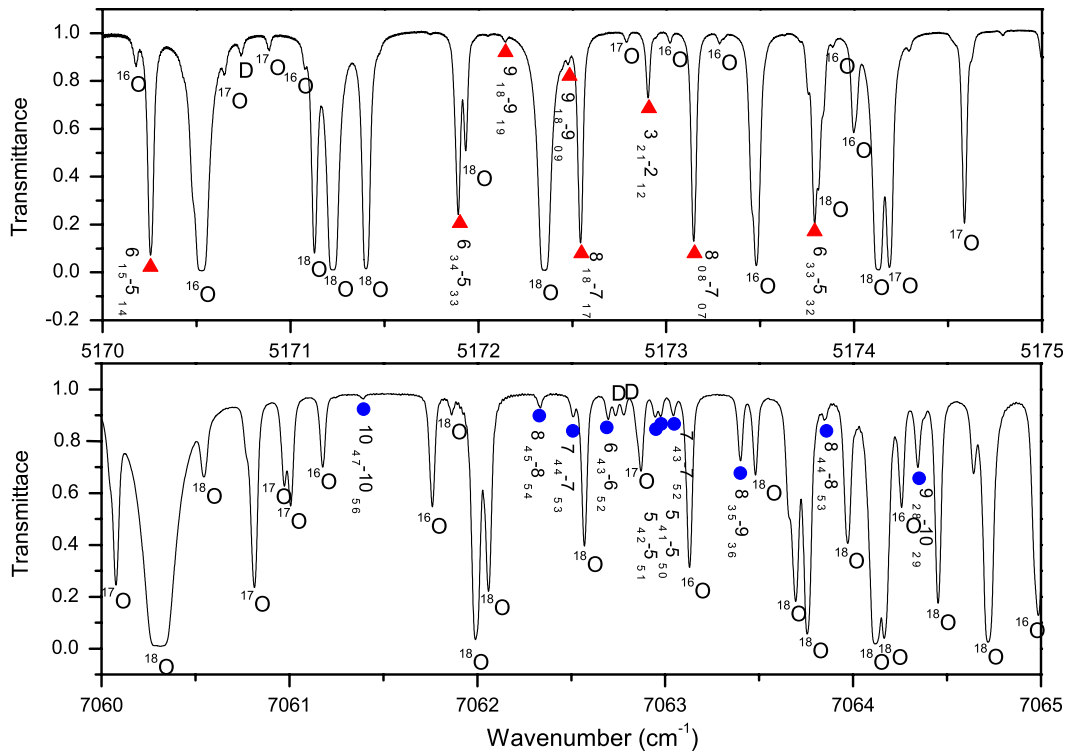

Fig. 2. A small part of the $HD^{18}O$ spectrum. (Upper panel) 5170–5175 cm^{-1} region of the $\nu_2 + \nu_3$ band recorded with InSb detector and 0.01 cm^{-1} unapodized resolution. (Lower panel) 7060–7065 cm^{-1} region of the $2\nu_3$ band recorded at 0.015 cm^{-1} unapodized resolution. Experimental conditions: absorption path length 105 m, sample pressure 1307 Pa. Lines marked with ^{16}O, ^{18}O, ^{17}O, and D are due to $H_2{}^{16}O$, $H_2{}^{18}O$, $H_2{}^{17}O$, and $HD^{16}O$, respectively.

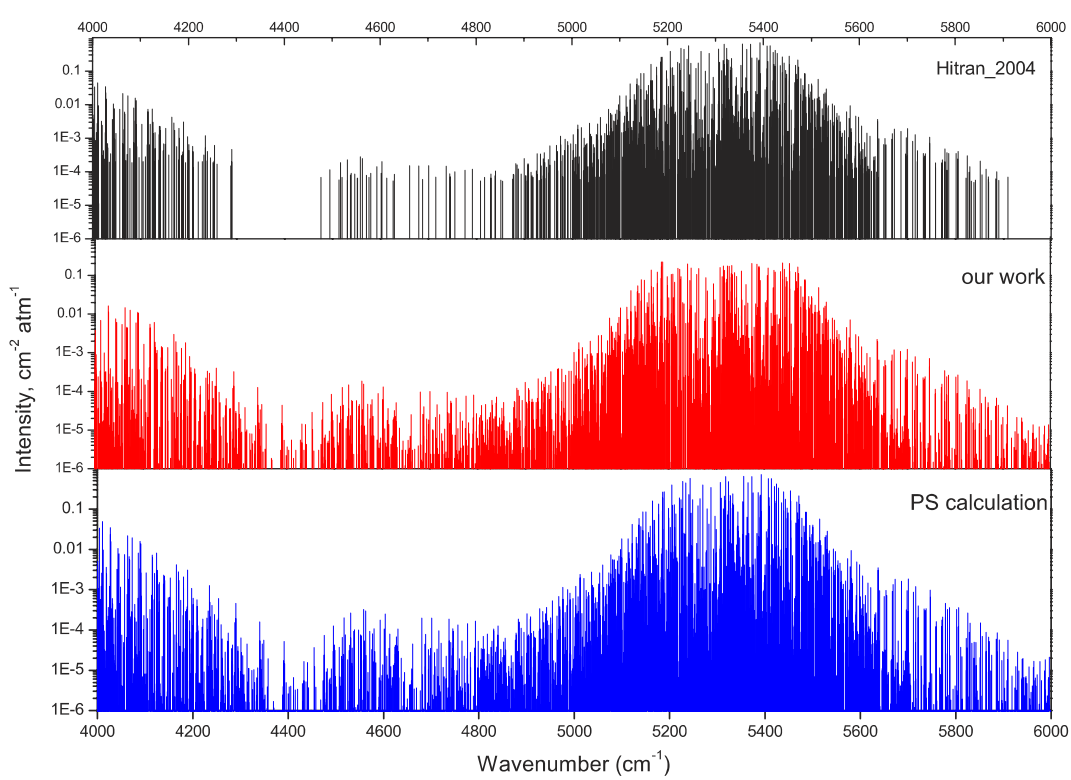

Fig. 3. $H_2{}^{18}O$ stick spectrum from HITRAN2004 database, Schwenke and Partridge calculations [30,31] and this work.

determine the real isotopic concentration of the sample used in our measurements. As discussed in [27], the isotope abundance of $H_2{}^{18}O$ in each spectrum were estimated by the comparison of the line intensities (retrieved from line profile fittings to our spectrum) of some "moderate" lines with their values given in the HITRAN2004 database. Then this isotopic abundance value from each spectrum will be used to determine the intensities of other lines. The intensities in this work were derived as in [27]. The precision of the intensities of well isolated and not-very-weak $H_2{}^{18}O$ lines is estimated to be about 15% which should mainly comes from the ambiguity of the partial pressure of the sample.

3. Spectral analysis and results

3.1. $H_2{}^{18}O$

With the help of the high accurate calculations by Schwenke and Partridge [30,31], the observed lines of $H_2{}^{18}O$ in the first and second hexade region [27,28] have been successfully assigned. Seven bands of $H_2{}^{18}O$ locate in the 1080–6000 cm^{-1} region: ν_2, ν_1, $2\nu_2$, ν_3, $\nu_1+\nu_2$, $3\nu_2$, and $\nu_2+\nu_3$. The assignments of the $H_2{}^{18}O$ lines in this region were done straightforwardly by the identification procedure in a similar way. The final $H_2{}^{18}O$ identification list is attached to the paper as the Supplementary Material I, which includes 5031 lines corresponding to 5234 transitions. For each line, the experimental and PS calculated intensities are given followed by ro-vibrational assignments. It also contains some $H_2{}^{18}O$ lines superimposed by the transitions of other water isotopes, these lines are specially marked in the list.

In a new version of HITRAN2004, there are 4297 transitions stronger than $2.5\times10^{-5}cm^{-1}/(atm\ cm)$ assigned to $H_2{}^{18}O$ in the studied region. The detection limit of the spectrum presented in this work extends to about $10^{-6}\ cm^{-1}/(atm\ cm)$. On the one hand, there are 1300 transitions included in HITRAN2004 database but

Table 2
Summary of the determined energy levels of $H_2{}^{18}O$

V	J^{max}	K_a^{max}	Number of levels			
			This work	[34]	New	Diff
010	20	10	205	192	32	26
020	16	10	148	98	50	2
100	15	10	197	126	71	3
001	19	11	223	161	62	3
030	15	8	117	3	114	0
110	15	8	147	102	46	7
011	18	10	209	153	57	10
021	11	7	75	90		
120	9	4	18	59		
Total			1339	984	432	51

Table 3
New ro-vibrational energy levels of $H_2{}^{18}O$ (cm^{-1})

V	J	K_a	K_c	E	δ	N
010	11	10	2	4730.2169		1
010	11	10	1	4730.2171		1
010	12	8	4	4528.0225		1
010	12	9	4	4769.5012	0.7	2
010	12	9	3	4769.5012	0.7	2
010	12	10	3	5024.7743		1
010	12	10	2	5024.7743		1
010	13	6	8	4416.2162	0.8	3
010	13	7	7	4618.0661		1
010	13	7	6	4618.6401	0.6	3
010	13	8	6	4842.0717		1
010	13	8	5	4842.1121		1
010	14	4	10	4511.3382		1
010	14	5	9	4623.2336		1
010	14	6	9	4752.4738		1
010	14	6	8	4764.7951		1
010	14	7	8	4954.6021		1
010	15	4	12	4717.4724	0.1	2
010	15	4	11	4879.1616		1
010	16	2	14	4827.4965		1
010	16	3	14	4827.8595		1
010	16	3	13	5069.8538		1
010	16	4	13	5073.9073		1
010	17	1	16	4882.2282		1
010	17	2	16	4882.2539		1
010	17	2	15	5183.4974		1
010	18	1	17	5236.7778		1
010	18	2	17	5236.7759		1
010	19	0	19	5220.0202		1
010	19	1	19	5220.0185		1
010	19	1	18	5608.6196		1
010	20	1	20	5588.0767		1
020	7	7	1	4780.7990	0.4	4
020	7	7	0	4780.7989	0.5	5
020	8	7	2	4977.3155	0.7	5
020	8	7	1	4977.3155	0.9	3
020	8	8	1	5225.4954		1
020	8	8	0	5225.4955		1
020	9	4	6	4579.8581	0.9	5
020	9	5	5	4759.7437	0.5	6
020	9	6	4	4967.2336	0.6	3
020	9	6	3	4966.5170	0.7	5
020	9	7	3	5197.6542		1
020	9	7	2	5197.6747	0.4	2
020	9	8	2	5447.0708		1
020	9	8	1	5447.0702		1
020	9	9	1	5709.4806		1
020	9	9	0	5709.4806		1
020	10	2	8	4626.9621	0.2	3
020	10	3	7	4735.8014	0.3	2
020	10	4	7	4821.0840	0.5	7
020	10	4	6	4844.7631		1
020	10	5	6	5002.9269	0.6	3
020	10	5	5	5005.8557	0.5	4
020	10	6	5	5210.5721		1
020	10	6	4	5209.9748		1
020	10	7	4	5441.5891		1
020	10	9	2	5956.1109		1
020	11	2	10	4697.2244	0.6	4
020	11	2	9	4887.0990	0.4	5
020	11	3	9	4902.0883	0.9	3

Note. N is the number of lines used for the upper level determination and δ denotes the experimental uncertainties (combination differences) in $10^{-3}\ cm^{-1}$.

Table 3 (*continued*)

V	J	K_a	K_c	E	δ	N
020	11	3	8	5016.8388		1
020	11	4	8	5084.1590	0.2	2
020	11	4	7	5124.9905		1
020	11	5	7	5269.4179		1
020	11	5	6	5276.3759	0.4	2
020	12	1	11	4946.5352	0.5	4
020	12	2	10	5162.8585	0.0	2
020	12	4	9	5367.7776		1
020	12	4	8	5431.5156		1
020	12	5	8	5557.6643		1
020	13	1	12	5214.6887	0.3	3
020	13	2	12	5215.1013		1
020	13	2	11	5455.5986		1
020	13	3	11	5461.0621		1
020	13	3	10	5635.5471		1
020	14	0	14	5182.9217	0.6	2
020	14	1	14	5182.9219	0.3	3
020	14	3	12	5767.1183		1
020	15	3	12	6322.1378		1
020	16	0	16	5758.0375		1
020	16	1	16	5758.0380		1
100	9	8	2	5595.7977	0.3	2
100	9	8	1	5595.7975	0.7	2
100	9	9	1	5803.1037	1.0	2
100	9	9	0	5803.1038	0.9	2
100	10	6	4	5476.8202	0.9	4
100	10	7	3	5646.2254		1
100	10	8	3	5836.6874		1
100	10	8	2	5836.6890	0.3	2
100	10	9	2	6045.6389	0.9	2
100	10	9	1	6045.6393	0.8	2
100	10	10	1	6276.3779		1
100	10	10	0	6276.3757		1
100	11	3	9	5306.6933	0.2	4
100	11	4	8	5450.1317	0.5	2
100	11	7	5	5909.7285		1
100	11	7	4	5909.8120	1.4	2
100	11	8	4	6100.7209		1
100	11	8	3	6100.7245	1.0	4
100	11	9	3	6311.2599		1
100	11	9	2	6311.2594		1
100	11	10	2	6545.9418		1
100	11	10	1	6545.9421		1
100	12	1	11	5383.5255		1
100	12	2	10	5566.2336		1
100	12	3	10	5569.3091	0.1	2
100	12	3	9	5712.3794		1
100	12	4	9	5726.3086	0.6	4
100	12	5	8	5870.8142	0.6	3
100	12	5	7	5903.0037		1
100	12	6	6	6030.9186		1
100	12	7	6	6196.4569	0.1	2
100	12	7	5	6196.7270		1
100	12	8	5	6387.6796		1
100	12	8	4	6387.6944		1
100	12	9	4	6599.7013		1
100	12	9	3	6599.7004		1
100	13	1	12	5645.9614	0.7	2
100	13	2	12	5644.4435		1
100	13	2	11	5846.1445		1
100	13	3	11	5845.9216		1
100	13	3	10	6013.4969		1
100	13	4	10	6021.1418		1
100	13	4	9	6135.0728	0.3	2
100	13	5	9	6176.6638		1

Table 3 (*continued*)

V	J	K_a	K_c	E	δ	N
100	13	5	8	6226.8674		1
100	13	6	8	6341.5623		1
100	13	6	7	6345.4345		1
100	13	7	7	6506.2070		1
100	13	7	6	6506.9693		1
100	13	8	6	6697.3398		1
100	14	0	14	5674.6693		1
100	14	1	14	5674.6700	0.2	2
100	14	1	13	5923.3917		1
100	14	2	13	5923.5386		1
100	14	2	12	6143.5077		1
100	14	3	12	6142.7168		1
100	14	3	11	6330.2054		1
100	14	4	11	6333.9412		1
100	14	5	10	6502.0865		1
100	14	5	9	6575.1397		1
100	14	6	9	6656.6080	0.3	2
100	14	6	8	6685.8146		1
100	14	7	8	6838.7827		1
100	14	7	7	6840.6532		1
100	15	0	15	5952.8898	0.7	2
100	15	1	15	5952.8881		1
100	15	2	13	6455.7361		1
100	15	3	13	6456.4584		1
100	15	3	12	6663.1368		1
100	15	4	11	6829.7715		1
100	15	7	8	7198.1039		1
001	9	9	1	5858.8783	0.9	3
001	9	9	0	5858.8777	0.6	3
001	10	9	2	6101.8094	1.0	3
001	10	9	1	6101.8093	0.6	3
001	10	10	1	6313.4094		1
001	10	10	0	6313.4094		1
001	11	7	5	5984.0698	0.1	2
001	11	7	4	5984.2417	0.4	3
001	11	8	4	6167.6226	0.6	4
001	11	8	3	6167.6298		1
001	11	9	3	6367.8641	0.2	3
001	11	9	2	6367.8641	0.5	2
001	11	11	1	6804.8052		1
001	11	11	0	6804.8052		1
001	12	7	6	6271.9621	0.2	3
001	12	7	5	6272.5146	0.3	3
001	12	8	5	6455.6141	0.9	2
001	12	8	4	6455.6457		1
001	12	9	4	6656.7743	1.3	2
001	12	9	3	6656.7719	0.9	3
001	13	5	8	6316.4003	0.4	2
001	13	6	8	6418.7810	0.4	2
001	13	6	7	6431.2897	0.1	2
001	13	7	7	6582.9093	0.1	2
001	13	7	6	6584.4453	1.1	2
001	13	8	6	6766.4270	0.8	2
001	13	8	5	6766.5438		1
001	14	3	12	6239.6337	0.0	2
001	14	3	11	6426.9046		1
001	14	4	11	6429.7520	0.6	3
001	14	4	10	6573.8670	0.8	2
001	14	5	10	6595.3178		1
001	14	5	9	6683.1843	0.3	2
001	14	6	9	6751.3228		1
001	14	6	8	6774.9442		1
001	14	7	7	6920.3004	0.2	2
001	14	8	6	7100.2245		1
001	15	1	14	6318.4331		1

(*continued on next page*)

Table 3 (*continued*)

V	J	K_a	K_c	E	δ	N
001	15	2	13	6553.1338	0.5	2
001	15	3	13	6554.1362	0.8	2
001	15	3	12	6759.1130	1.7	2
001	15	4	12	6760.9274	0.7	2
001	15	4	11	6928.0323		1
001	15	5	11	6940.9377	0.2	2
001	15	5	10	7051.6455		1
001	15	6	10	7104.8934	1.5	2
001	16	1	15	6633.1669		1
001	16	2	15	6633.1421		1
001	16	2	14	6885.5872	0.8	2
001	16	3	13	7108.2041		1
001	16	4	13	7109.2586		1
001	16	4	12	7297.0275		1
001	17	1	17	6663.9213		1
001	17	1	16	6965.0865		1
001	17	2	16	6965.0608		1
001	17	3	15	7234.3224		1
001	18	0	18	6995.3560	0.8	2
001	18	1	18	6995.3568		1
001	18	1	17	7314.2251		1
001	18	2	17	7314.2271		1
001	19	0	19	7344.0732		1
001	19	1	19	7344.0749		1
030	0	0	0	4648.4771		1
030	1	0	1	4672.2266	0.5	4
030	1	1	1	4698.5317	0.2	3
030	1	1	0	4704.6302	0.5	3
030	2	0	2	4718.7411	0.6	4
030	2	1	2	4739.9705	0.4	7
030	2	1	1	4758.2324	0.1	4
030	2	2	1	4834.6627	0.1	5
030	2	2	0	4835.6053	0.3	5
030	3	0	3	4786.2349	0.2	4
030	3	1	3	4801.5276	0.7	5
030	3	1	2	4837.8491	0.5	6
030	3	2	2	4906.0978	1.0	8
030	3	2	1	4910.6282	0.6	8
030	3	3	1	5042.1397	0.4	4
030	3	3	0	5042.2364	0.7	6
030	4	0	4	4872.7137	0.5	3
030	4	1	4	4882.6337	0.7	7
030	4	1	3	4942.4425	0.8	5
030	4	2	3	5000.4339	0.4	7
030	4	2	2	5013.0632	0.9	6
030	4	3	2	5139.2836	0.5	6
030	4	3	1	5139.9384	0.6	5
030	4	4	1	5315.6843	0.6	5
030	4	4	0	5315.6940	1.0	3
030	5	0	5	4976.7851	0.6	5
030	5	1	5	4982.7216	0.2	3
030	5	1	4	5070.4971	0.9	5
030	5	2	4	5116.9576	0.4	5
030	5	2	3	5143.3763	0.3	7
030	5	3	3	5260.6654	1.0	7
030	5	3	2	5263.1536	0.6	6
030	5	4	2	5437.5894	0.8	4
030	5	4	1	5437.6654	0.8	6
030	5	5	1	5648.4248		1
030	5	5	0	5648.4242	0.6	4
030	6	0	6	5097.9364		1
030	6	1	6	5101.3117	0.8	3
030	6	1	5	5220.0547	0.2	3
030	6	2	5	5254.8642	0.9	5
030	6	2	4	5300.9250	0.8	5
030	6	3	4	5405.9352	0.6	5

Table 3 (*continued*)

V	J	K_a	K_c	E	δ	N
030	6	3	3	5412.8464	0.8	4
030	6	4	3	5583.8994	0.4	6
030	6	4	2	5584.2591	0.4	2
030	6	5	2	5795.1208	0.4	2
030	6	5	1	5795.1390	0.3	3
030	6	6	1	6034.0149	0.1	2
030	6	6	0	6034.0113		1
030	7	0	7	5236.1776	0.4	3
030	7	1	7	5238.0483		1
030	7	1	6	5389.0007	0.2	3
030	7	2	6	5413.3323	0.2	2
030	7	2	5	5484.2764		1
030	7	3	5	5574.5217	0.4	3
030	7	3	4	5589.9910	0.8	4
030	7	4	4	5754.4955	0.5	4
030	7	4	3	5755.7185	0.6	5
030	7	5	3	5966.0254	1.4	2
030	7	5	2	5966.1099	0.5	3
030	7	6	1	6205.7837		1
030	7	7	1	6466.6353		1
030	7	7	0	6466.6353	0.2	2
030	8	0	8	5391.6628		1
030	8	1	8	5392.6929	0.8	2
030	8	1	7	5575.6122	0.2	2
030	8	2	7	5591.5935	0.0	2
030	8	2	6	5691.5536	0.4	2
030	8	3	6	5765.6660	0.1	4
030	8	3	5	5795.0399	0.1	2
030	8	4	5	5949.1204	0.3	4
030	8	4	4	5952.7443		1
030	8	5	4	6160.9929	0.4	2
030	8	5	3	6161.2749		1
030	8	6	3	6401.5706		1
030	8	6	2	6401.6196		1
030	8	7	2	6663.4199		1
030	8	8	1	6940.7546		1
030	8	8	0	6940.7552		1
030	9	0	9	5564.5200	0.9	2
030	9	1	9	5565.0884		1
030	9	1	8	5778.9779	0.1	2
030	9	2	8	5788.9918	0.3	2
030	9	2	7	5920.6215	0.6	3
030	9	3	7	5978.4992		1
030	9	3	6	6027.4123	1.2	2
030	9	4	5	6175.3114	0.4	3
030	9	5	4	6380.5079	1.0	3
030	9	6	4	6621.2067		1
030	9	6	3	6621.4141		1
030	9	7	2	6883.8908		1
030	9	8	2	7162.4959		1
030	9	8	1	7162.5014		1
030	10	0	10	5754.8207		1
030	10	1	10	5755.1393	0.4	2
030	10	1	9	5998.9263	0.2	2
030	10	2	9	6005.0197	0.6	2
030	10	3	8	6212.0999	0.4	2
030	10	4	7	6408.4893		1
030	10	4	6	6424.7012		1
030	10	6	5	6864.5129		1
030	11	0	11	5962.6038	0.4	2
030	11	1	11	5962.7868		1
030	11	1	10	6235.6571		1
030	11	6	6	7131.4893		1
030	11	6	5	7134.5964		1
030	12	1	12	6187.9856		1
030	12	2	10	6717.1354		1

Table 3 (*continued*)

V	J	K_a	K_c	E	δ	N
030	12	3	10	6741.2305		1
030	12	4	9	6954.6075		1
030	12	5	8	7183.6783		1
030	12	6	7	7421.4187		1
030	13	2	11	7016.9270		1
030	13	6	8	7733.0660		1
030	14	2	12	7332.7516		1
030	14	3	12	7339.8673	0.7	2
030	15	3	12	7895.5905		1
110	7	7	1	6684.3091		1
110	7	7	0	6684.3093		1
110	8	6	2	6681.6467		1
110	8	7	2	6877.8207	0.4	3
110	8	7	1	6877.8156		1
110	8	8	1	7094.6902	0.8	2
110	8	8	0	7094.6900		1
110	9	6	4	6898.1457	1.7	2
110	9	7	3	7094.9237		1
110	9	7	2	7094.9249	0.2	2
110	9	8	1	7313.2128		1
110	10	2	8	6654.1277		1
110	10	3	7	6758.8410	0.8	2
110	10	4	6	6844.3094	0.4	3
110	10	5	5	6970.3475	0.8	3
110	10	6	5	7138.3040	0.3	2
110	10	6	4	7138.6208		1
110	10	7	4	7335.4278		1
110	10	7	3	7335.4436		1
110	10	8	3	7555.0455		1
110	11	2	10	6727.6103		1
110	11	3	9	6912.2515		1
110	11	3	8	7031.9419	0.7	2
110	11	4	8	7069.0548	0.4	2
110	11	4	7	7119.7293	0.0	1
110	11	6	6	7401.9120	1.7	2
110	11	6	5	7402.8466	0.6	2
110	11	7	5	7599.1322		1
110	11	7	4	7599.1874		1
110	11	8	3	7819.9198		1
110	12	1	11	6971.1986		1
110	12	2	11	6973.6685	0.0	2
110	12	2	10	7170.2513		1
110	12	4	9	7346.8085		1
110	12	5	7	7534.7083		1
110	12	6	6	7691.1132		1
110	12	7	6	7885.8216		1
110	13	0	13	6974.4174	1.1	2
110	13	1	13	6974.5341		1
110	13	1	12	7233.7194		1
110	13	5	9	7815.6391		1
110	14	0	14	7232.7676		1
110	14	1	14	7232.7672		1
110	14	2	13	7510.6075		1
110	15	0	15	7508.1380		1
110	15	1	15	7508.1374		1
011	9	9	1	7584.6735	0.9	2
011	9	9	0	7584.6723	0.0	2
011	10	5	6	7045.0169	0.1	2
011	10	7	4	7398.3291	0.1	2
011	10	7	3	7398.3547	0.8	5
011	10	8	3	7605.8516	0.7	4
011	10	8	2	7605.8519	0.6	4
011	10	9	2	7828.9125	1.0	2
011	10	9	1	7828.9137	0.0	2
011	10	10	1	8063.7998		1
011	10	10	0	8063.7998		1

Table 3 (*continued*)

V	J	K_a	K_c	E	δ	N
011	11	7	4	7663.5261	0.3	3
011	11	8	4	7871.6578		1
011	11	8	3	7871.6583		1
011	11	9	3	8096.1766		1
011	11	9	2	8096.1766		1
011	12	7	6	7951.6604	0.1	2
011	12	7	5	7951.9839	0.3	2
011	12	8	5	8160.3663		1
011	12	8	4	8160.3681	0.9	2
011	12	9	3	8386.1401	0.0	2
011	13	3	10	7722.2838	0.8	2
011	13	4	9	7850.5614	0.4	2
011	13	5	8	7947.1728	1.4	2
011	13	6	8	8074.7710	1.3	2
011	13	6	7	8083.3053		1
011	13	7	7	8262.7641	0.1	2
011	13	7	6	8263.6447		1
011	13	8	6	8471.6543		1
011	14	3	12	7845.1412		1
011	14	3	11	8043.7642	1.4	2
011	14	4	11	8051.1389		1
011	14	4	10	8194.0785	0.5	2
011	14	5	10	8232.2211		1
011	14	5	9	8296.6317		1
011	14	6	9	8407.7967		1
011	14	6	8	8424.7167		1
011	14	7	7	8598.6700		1
011	15	1	14	7902.6592		1
011	15	2	14	7904.6964	1.4	2
011	15	2	13	8159.6625		1
011	15	3	13	8161.1956		1
011	15	3	12	8380.5136		1
011	15	4	12	8384.8069		1
011	15	4	11	8554.2435		1
011	15	5	11	8579.7038		1
011	15	6	10	8762.0454		1
011	16	1	16	7900.3385	0.8	2
011	16	1	15	8217.2587		1
011	16	2	15	8217.1817		1
011	16	2	14	8493.4962		1
011	16	3	14	8494.5579		1
011	16	3	13	8732.9250		1
011	17	0	17	8211.4060		1
011	17	1	17	8211.4070		1
011	17	2	16	8548.8697		1
011	18	0	18	8539.6131		1

not given in our linelist (Supplemental Material I) because they are too strong or blended by adjacent lines. On the other hand, totally 2341 new transitions were observed. In particular 330 transitions of the $3\nu_2$ band were obtained. Moreover, 93 lines show large disagreement between the values in HITRAN2004 and in this work, 87 of them are listed in HITRAN2004 but not evidenced in our spectrum. The largest deviation is up to $-9.3\ \mathrm{cm}^{-1}$. It implies that some mis-assigned or poorly simulated lines in this region remain in the HITRAN2004 database. These transitions together with our assignments can be found in the Supplemental Material I attached to this paper.

In the PS calculation, 8824 transitions of $H_2{}^{18}O$ are predicted to be stronger than $1.0 \times 10^{-6}\ cm^{-1}/(atm\ cm)$ in the studied region including hot transitions. The data of HITRAN2004 database in the studied region comes from Refs. [12,17–19,22]. Owing to relatively longer absorption path length and higher partial pressure of the $H_2{}^{18}O$ sample in our experiment, we observed more weak lines. While in some regions, many strong lines are saturated. Together with previous work, totally 6534 transitions have been observed. With very careful comparison with the observations and predictions, we think the remainder are blended by other strong transitions of $H_2{}^{18}O$ or other isotopologues of water. Fig. 3 shows the stick spectrum in 4000–6000 cm^{-1} region provided by this work, HITRAN2004, and PS calculation. Obviously there are much more transitions contained in this work than in HITRAN2004, and our results agree well with the PS calculations.

Table 2 gives a summary of $H_2{}^{18}O$ energy levels determined in this work. The result given by [34] is also presented as a comparison. In this work, totally 1339 rotational energy levels of 9 different upper vibrational states were determined, while the number is 432 from [34]. In particular, the rotational energy levels of the (030) state are mostly obtained for the first time. The complete list of the energy levels is given in Supplementary Material II attached to this paper. Only the newly derived energy levels are given in Table 3 here. Totally 946 energy levels were confirmed through combination differences of two or more transitions. The average experimental uncertainty for these levels was estimated to be about 0.0005 cm^{-1}. According to the systematic tendency of the $E_{obs-calc}$ values (difference between observed and PS predicted energies) and the line intensity predictions, energy levels derived from one transition can be validated, but may have considerably larger uncertainty. Besides of 432 new energy levels, 51 energy levels are very different from those in [34]. For these very different levels, 44 of them given in [34] have large uncertainties (up to 0.03 cm^{-1}), some rise up from transitions do not appear in our spectrum, which could be in error. For our derivation of such levels, they are confirmed by the comparison with the PS calculations (both line positions and intensities), and 39 of them even with good combination differ-

Table 4
$H_2{}^{18}O$ energy levels which is much different with those in [34]

V	J	K_a	K_c	This work			Ref. [34]	
				E	δ	N	E	δ
010	10	9	2	4207.2975	0.64	4	4208.520220	0.4
010	10	9	1	4207.2970		1	4208.520220	0.4
010	10	10	1	4458.5028	1.03	2	4467.825950	3.0
010	10	10	0	4458.5016	0.07	2	4467.825950	3.0
010	11	6	5	3812.6606	0.23	4	3812.680000	3.0
010	11	9	3	4476.9332		1	4477.870600	3.0
010	11	9	2	4476.9331	0.59	3	4477.870600	3.0
010	12	4	8	3831.1147	0.68	5	3831.070000	3.0
010	12	6	7	4102.4117	0.28	4	4102.043100	4.0
010	12	6	6	4105.0445	0.58	5	4104.731430	4.0
010	12	7	6	4304.3001	0.42	5	4303.652600	2.0
010	12	7	5	4304.5020	0.63	3	4303.866220	4.0
010	12	8	5	4528.0136	0.95	2	4527.266900	4.0
010	13	4	9	4161.1780	0.02	3	4160.835570	2.0
010	13	5	9	4234.4176	0.34	3	4234.005880	4.0
010	13	5	8	4270.2918	0.59	5	4270.018360	2.0
010	13	6	7	4422.2331	0.44	4	4421.703200	3.0
010	14	2	12	4166.6145	0.20	2	4166.661910	3.0
010	14	3	11	4366.8762	0.49	2	4366.483400	3.0
010	14	5	10	4566.5879	0.54	2	4565.874270	4.0
010	15	3	13	4489.1903		1	4489.390050	4.0
010	15	3	12	4710.5253	0.91	2	4710.032710	4.0
010	16	1	15	4545.1661		1	4545.295700	4.0
010	16	2	15	4545.1537		2	4545.313200	4.0
010	18	0	18	4869.1798		1	4869.249500	4.0
010	18	1	18	4869.1798		1	4869.249500	4.0
020	7	5	3	4345.1004	0.53	5	4345.138720	0.4
020	13	1	13	4921.6103		1	4921.599000	3.0
100	10	7	4	5646.2033	0.42	3	5646.200880	3.0
100	11	2	9	5303.2254		1	5303.231280	0.8
100	11	3	8	5426.8684	0.61	3	5426.864710	1.0
001	8	7	2	5261.0099		1	5261.003740	1.0
001	12	1	12	5268.4148		1	5268.430300	3.0
001	13	4	9	6235.1536	0.22	3	6235.079880	0.4
110	3	2	2	5433.5423	0.58	5	5433.550180	0.2
110	4	4	0	5736.5663	0.40	2	5736.577300	1.0
110	6	5	2	6147.7326	0.36	6	6147.735200	1.5
110	8	5	4	6509.1524	0.71	6	6509.147450	1.5
110	10	5	6	6966.6160	0.71	5	6966.611540	1.5
110	11	5	7	7232.1400	0.72	3	7232.137800	2.0
110	11	5	6	7239.2275		1	7239.378400	5.0
011	9	7	2	7156.5940	0.80	2	7156.588300	0.4
011	12	1	12	6829.2725		1	6829.277900	3.0
011	12	4	8	7527.2949	0.18	3	7527.291470	1.5
011	12	5	8	7596.1095	0.59	3	7596.104500	2.0
011	12	6	6	7767.5980	0.43	3	7767.611000	2.0
011	13	2	11	7545.1740	0.68	2	7545.178120	1.5
011	14	1	14	7328.0896	0.73	2	7330.408100	3.0
011	14	1	13	7606.5469	1.00	4	7606.542530	1.5
011	14	2	13	7606.1635	0.47	2	7606.157500	2.0
011	16	0	16	7900.3387	1.02	2	7900.286400	2.0

Note. N is the number of lines used for the upper level determination and δ denotes the experimental uncertainties (combination differences) in $10^{-3}\ cm^{-1}$.

Table 5
Summary of the determined energy levels of $HD^{18}O$

V	E_v (cm^{-1})	J^{max}	K_a^{max}	Number of Levels			Number of Transitions
				This work	Ref. [34]	New	
010	1396.267	18	9	182	137	47	807
100	2709.284	14	7	127	105	24	632
020	2767.212	12	6	91	59	32	500
001	3696.330	17	9	163	128	36	891
110	4080.545	14	6	101	83	18	458
030	4121.754	12	4	76	55	21	331
011	5071.497	14	8	121	0	121	891
200	5335.361	13	5	77	0	77	172
002	7229.186	14	7	128	0	128	523
Total				1066	567	504	4942

Table 6
New $HD^{18}O$ ro-vibrational energy levels of the (010), (020), (100), and (001) states (cm^{-1})

V	J	K_a	K_c	E	δ	N
010	8	8	0	2991.1921	0.1	2
010	8	8	1	2991.1921	0.1	2
010	9	8	1	3128.7208	0.4	2
010	9	8	2	3128.7208	0.4	2
010	9	9	0	3386.0115		1
010	9	9	1	3386.0115		1
010	10	7	3	3050.7079	1.7	2
010	10	7	4	3050.7093	0.1	2
010	10	8	2	3281.5131	0.1	3
010	10	8	3	3281.5135	0.4	3
010	10	9	1	3537.9484		1
010	10	9	2	3537.9484		1
010	11	6	5	3017.0810	1.1	2
010	11	6	6	3017.0468	0.6	2
010	11	7	4	3219.7376		1
010	11	7	5	3219.7374		1
010	11	8	3	3449.5420		1
010	11	8	4	3449.5419		1
010	12	3	9	2816.5719	1.2	5
010	12	4	8	2901.2141	0.7	2
010	12	4	9	2885.6902	0.6	4
010	12	5	7	3032.0004	1.5	2
010	12	5	8	3030.3640	0.7	2
010	12	6	6	3202.8245	0.9	2
010	12	7	5	3404.1541		1
010	12	7	6	3404.1531		1
010	13	3	10	3030.7361	0.9	4
010	13	3	11	2951.8042	0.7	3
010	13	4	9	3113.0114	0.9	3
010	13	4	10	3087.6435	0.1	2
010	13	5	9	3233.0517	0.5	2
010	14	1	13	2999.1195*	0.4	4
010	14	2	12	3152.3001		1
010	14	2	13	2999.7157*	1.0	3
010	14	3	11	3259.1276		1
010	14	3	12	3160.5271	0.3	2
010	14	4	10	3342.4247		1
010	14	4	11	3304.0607		1
010	15	1	14	3500.6075		1
010	15	2	14	3208.3146	0.5	2
010	15	3	12	3207.9880	0.5	2
010	15	3	13	3382.0060		1
010	15	4	11	3588.7506		1
010	16	1	15	3754.1234		1
010	17	0	17	3431.5413	1.2	2
010	17	1	17	3431.5413	1.2	2
010	17	2	15	4128.1632		1
010	18	0	18	3662.4399	0.6	2
010	18	1	18	3662.4399	0.6	2
020	4	2	3	3000.9061*	0.6	7
020	5	2	4	3077.5223*	0.5	10
020	5	4	1	3310.2743*	0.5	4
020	5	4	2	3310.2606*	1.1	4
020	5	5	0	3476.5602	1.5	2
020	5	5	1	3476.5574	0.1	2
020	6	2	4	3188.6710*	0.4	6
020	6	3	4	3271.5497*	0.6	7
020	6	4	2	3404.0529	1.2	3
020	6	4	3	3403.9936	0.4	5
020	6	5	1	3569.7720	0.7	2
020	6	5	2	3569.7691	0.6	2
020	6	6	0	3765.5563		1

Table 6 (*continued*)

V	J	K_a	K_c	E	δ	N
020	6	6	1	3765.5563		1
020	7	4	3	3513.7604	0.8	4
020	7	4	4	3513.5185	0.4	6
020	7	5	2	3678.6335		1
020	7	5	3	3678.6323		1
020	8	2	6	3440.6608*	0.4	4
020	8	3	5	3515.8779	0.6	5
020	8	3	6	3506.1184	0.6	5
020	8	4	4	3639.5768	0.3	4
020	8	4	5	3638.8755	0.5	3
020	9	2	7	3591.0107	0.8	5
020	9	2	8	3526.7059*	0.6	6
020	9	3	6	3663.7908	0.7	5
020	9	3	7	3646.2080	0.7	5
020	9	4	5	3781.7934	1.0	5
020	9	4	6	3780.0460	0.7	3
020	10	1	9	3665.3693	0.5	3
020	10	2	8	3756.3812	0.2	2
020	10	2	9	3672.9135	0.6	4
020	10	3	7	3829.6595		1
020	10	3	8	3801.0517	1.0	4
020	11	0	11	3672.5174	0.4	4
020	11	1	10	3827.3595	0.3	2
020	11	1	11	3672.7066	0.9	4
020	11	2	10	3832.0507	1.0	4
020	12	0	12	3829.1443	1.1	2
020	12	1	12	3829.2428	0.3	2
100	6	5	2	3402.4632*	0.8	3
100	8	7	1	3976.9806	0.1	2
100	8	7	2	3976.9806	0.1	2
100	9	6	3	3924.7221	1.2	3
100	9	6	4	3924.7211	1.8	4
100	10	1	9	3573.8685*	0.9	6
100	10	4	7	3789.7069*	0.2	3
100	10	5	5	3919.2559	0.2	3
100	10	5	6	3918.9716	1.0	3
100	10	6	4	4075.8407	1.1	2
100	11	2	9	3824.4797	1.3	4
100	11	2	10	3734.0784	0.6	4
100	11	3	8	3887.9070	0.8	2
100	11	3	9	3846.7062	1.1	4
100	11	4	7	3966.3054	0.8	3
100	11	4	8	3957.7405	0.9	3
100	11	5	6	4087.2614		1
100	11	5	7	4086.5306	0.0	2
100	12	1	11	3900.9751	0.8	4
100	12	2	10	4009.5552	0.9	4
100	12	2	11	3902.4388	0.3	3
100	12	3	9	4081.5967	0.3	3
100	12	3	10	4025.0022	0.7	3
100	13	0	13	3927.6035*	1.1	3
100	13	1	13	3927.6035*	1.1	3
100	13	2	11	4206.3337	0.4	2
100	13	2	12	4083.2118	0.9	3
100	14	0	14	4107.9437		1
100	14	1	14	4107.9608		1
001	10	3	8	4671.2933*	1.0	6
001	10	6	4	5044.4824	0.3	2
001	10	6	5	5044.4647	1.1	3
001	10	7	3	5217.9254	0.4	2
001	10	7	4	5217.9276	1.8	3
001	10	8	2	5415.9356	1.6	2
001	10	8	3	5415.9357	1.6	2
001	10	9	1	5637.4394	1.4	2

(*continued on next page*)

Table 6 (*continued*)

V	J	K_a	K_c	E	δ	N
001	10	9	2	5637.4394	1.4	2
001	11	4	7	4956.9408	1.5	4
001	11	4	8	4945.2065		1
001	11	5	6	5068.2171	0.7	3
001	11	5	7	5067.0483		1
001	11	6	5	5213.6119		1
001	11	6	6	5213.5497	0.0	2
001	11	7	4	5385.9305		1
001	11	7	5	5385.9303		1
001	12	1	11	4893.3999*	0.0	2
001	12	2	10	5006.2227	1.0	4
001	12	3	9	5081.7725		1
001	12	3	10	5017.2449	1.6	3
001	12	4	8	5150.7580	1.0	3
001	12	4	9	5130.5093	1.7	2
001	12	5	7	5255.5903		1
001	13	2	11	5203.2065	1.1	2
001	13	3	10	5075.4038	0.7	2
001	13	3	11	5210.0618	1.5	3
001	13	4	9	5362.1813		1
001	13	4	10	5330.3069		1
001	14	2	12	5411.5676	1.2	2
001	14	2	13	5269.7835		1
001	14	3	11	5269.5363		1
001	14	3	12	5415.6432	0.7	2
001	15	0	15	5294.8465*	0.5	2
001	15	1	14	5752.1256		1
001	15	1	15	5294.8477*	0.8	2
001	16	0	16	5500.5313	0.6	3
001	16	1	16	5500.5313	0.6	3
001	17	0	17	5718.3829	0.3	2
001	17	1	17	5718.3829	0.3	2

Note. N is the number of lines used for the upper level determination and δ denotes the experimental uncertainties (combination differences) in $10^{-3}\,\mathrm{cm}^{-1}$. Energy levels different from [34] are marked by '*'.

ences. Table 4 lists such energy levels which are very different with those in [34].

3.2. $HD^{18}O$

The isotopic abundance of $HD^{18}O$ molecule in the measurement with 1307 Pa sample was estimated to be about 0.8% by comparing the experimental line intensities of some moderate lines with the value given in [29]. In the 1080–7800 cm^{-1} region, there are 9 bands of $HD^{18}O$: ν_2, ν_1, $2\nu_2$, ν_3, $\nu_1+\nu_2$, $3\nu_2$, $\nu_2+\nu_3$, $2\nu_1$, and $2\nu_3$. There are also many lines due to $H_2{}^{18}O$, $H_2{}^{16}O$, and $HD^{16}O$ in this region. It makes the assignments of $HD^{18}O$ complicated. The line positions of $H_2{}^{16}O$ and $HD^{16}O$ can be known from HITRAN database and our previous measurements of the water sample. The new results of $H_2{}^{18}O$ presented in this paper are also used to identify the lines. All bands of $HD^{18}O$ studied in this work are found to be of the A/B hybrid type.

First, the experimental ground-state rotational energy levels of [34] were fitted with the Watson type Hamiltonian [35]:

$$\begin{aligned} H^v = {} & E^v + [A^v - \tfrac{1}{2}(B^v + C^v)]J_z^2 + \tfrac{1}{2}(B^v + C^v)J^2 + \tfrac{1}{2}(B^v - C^v)J_{xy}^2 \\ & - \Delta_K^v J_z^4 - \Delta_{JK}^v J_z^2 J^2 - \Delta_J^v J^4 - \delta_K^v \left[J_z^2, J_{xy}^2\right]_+ - 2\delta_J^v J^2 J_{xy}^2 + H_K^v J_z^6 \\ & + H_{KJ}^v J_z^4 J^2 + H_{JK}^v J_z^2 J^4 + H_J^v J^6 + \left[J_{xy}^2, h_K^v J_z^4 + h_{JK}^v J^2 J_z^2 + h_J^v J^4\right]_+ \\ & + L_K^v J_z^8 + L_{KKJ}^v J_z^6 J^2 + L_{JK}^v J_z^4 J^4 + L_{KJJ}^v J_z^2 J^6 + L_J^v J^8 \\ & + \left[J_{xy}^2, l_K^v J_z^6 + l_{KJ}^v J^2 J_z^4 + l_{JK}^v J^4 J_z^2 + l_J^v J^6\right]_+ \\ & + P_K^v J_z^{10} + \left[J_{xy}^2, p_K^v J_z^8\right]_+ + \ldots, \end{aligned} \tag{1}$$

where $J_{xy}^2 = J_x^2 - J_y^2$ and $[A,B]_+ = AB + BA$. The ground state constants were obtained with $1.95\times10^{-4}\,\mathrm{cm}^{-1}$ standard deviation, which can reproduce the experimental values pretty well. So a set of the ground state rotational energy levels was formed by calculated values. Actually, the analysis of ν_2, ν_1, ν_3, $2\nu_2$, $3\nu_2$, and $\nu_1+\nu_2$ bands were almost straightforward based on the previous work of Toth [34]. More assignments and energy levels have been obtained and used to refine the spectroscopic parameters. The $\nu_2+\nu_3$, $2\nu_1$, and $2\nu_3$ bands are observed for the first time, and they are strongly mixed with the absorptions of other isotopes of water. So these three bands were analyzed simultaneously with the determination of the Hamiltonian parameters in the "snow ball" method [36]. Table 5 gives a summary of assignments and energy levels obtained in this work and [34].

From 4942 transitions, 1062 final rotational energy levels of nine upper states were determined. The whole list can be found in Supplemental Material II. Tables 6 and 7 only give new derived energy levels. Rotational energy levels of $3\nu_2$ and $\nu_1+\nu_2$ states are all listed for convenience. Most energy levels were determined by two or more transitions from different ground state levels. δ (in $10^{-3}\,\mathrm{cm}^{-1}$), the experimental uncertainties which come from combination differences, and N, the number of lines used for the upper level determination are also presented in the same table. For most levels, δ values are less than $0.0012\,\mathrm{cm}^{-1}$, which represent the experimental accuracy. No transitions to 28 rotational energy levels in [34] are evidenced in our spectrum, 25 of them are replaced in this work. The ro-vibrational parameters of seven vibrational states (except (030) and (110)) were fitted by nonlinear least-squares method with Watson type Hamiltonian. The parameters are listed in Table 8. It is clear that these seven vibrational states can be treated well as isolated ones.

4. Conclusion

The high resolution Fourier-transform spectrum of ^{18}O enriched water vapor was recorded and analyzed in the 1080–7800 cm^{-1} spectral region. Analysis of the $3\nu_2$ band of $H_2{}^{18}O$ and the $\nu_2+\nu_3$, $2\nu_1$, and $2\nu_3$ bands of $HD^{18}O$ are reported for the first time. Totally 5231 and 4942 transitions were assigned to $H_2{}^{18}O$ and $HD^{18}O$, respectively. A set of 936 new accurate energy levels was derived for these two isopologues of water molecule.

Table 7
Full list of the ro-vibrational energy levels of the (110), (030), (011), (200), and (002) states of $HD^{18}O$ (in cm^{-1})

			(002)			(200)			(011)			(030)			(110)		
J	K_a	K_c	E	δ	N	E	δ	N	E	δ	N	E	δ	N	E	δ	N
	1		2	3	4	5	6	7	8	9	10	11	12	13	14	15	16
0	0	0	7229.1857		1	5335.3609		1	5071.4966	0.5	2	4121.7545	0.3	2	4080.5450		1
1	0	1	7244.4294	0.8	4	5350.2167	0.1	2	5086.8842	0.2	3	4137.1960	0.1	3	4095.8601	0.5	4
1	1	0	7259.2981	0.9	4	5366.6667		1	5104.6327	0.3	4	4159.5250	0.2	4	4117.3437	0.2	2
1	1	1	7256.4721	0.3	3	5364.1265		1	5101.6566	0.2	5	4156.4366	0.3	3	4114.3068	0.4	4
2	0	2	7274.4659	0.6	5	5379.6046	0.3	2	5117.2475	0.3	5	4167.7338	0.3	3	4126.1276	0.2	4
2	1	1	7292.5943	0.4	4	5398.9048	0.3	3	5138.3678	0.2	5	4193.5463	0.2	5	4150.9246	0.2	4
2	1	2	7284.1234	0.3	6	5391.2817		1	5129.4476	0.3	6	4184.2795	0.8	5	4141.8354	0.7	5
2	2	0	7329.0392	0.6	4	5440.7292		1	5182.8407	0.6	6	4253.5377	0.4	6	4203.4486	0.7	5
2	2	1	7328.5998	0.2	5	5440.4140		1	5182.4367	0.3	4	4253.2000	0.9	7	4203.0983	0.2	7
3	0	3	7318.4706	0.8	4	5422.9049	0.7	3	5161.8093	0.8	8	4212.7041	0.6	6	4170.6566	0.6	3
3	1	2	7342.2116	0.9	6	5447.0262	0.1	3	5188.6697	0.2	7	4244.3489	0.4	6	4201.0068	0.4	5
3	1	3	7325.3315	0.6	7	5431.8105	0.1	3	5170.8847	0.7	9	4225.8312	0.7	7	4182.9113	0.6	5
3	2	1	7376.3983	0.2	4	5486.4534	0.4	3	5230.5062	0.3	7	4301.3859	0.7	6	4250.4318	0.5	8
3	2	2	7374.2706	0.6	8	5484.9054		1	5228.5397	0.3	8	4299.7299	0.8	7	4248.7154	0.8	8
3	3	0	7441.2291	0.4	4	5560.0197	0.1	2	5308.8963	0.2	5	4409.3005	0.3	3	4337.5020	0.4	4
3	3	1	7441.1858	0.4	4	5559.9948	0.2	2	5308.8619	0.2	4	4409.2786	0.5	4	4337.4753	0.7	7
4	0	4	7375.4988	0.8	6	5479.3528	0.2	3	5219.6322	0.5	7	4271.2605	0.5	6	4228.5611	0.8	6
4	1	3	7407.6996	0.9	3	5510.7162	0.7	3	5255.1316	0.6	9	4311.6240	0.3	6	4267.2129	0.5	5
4	1	4	7379.8350	0.9	5	5485.5200	1.1	3	5225.7184	0.4	9	4280.8693	0.6	3	4237.3111	0.6	6
4	2	2	7440.7693	1.0	5	5548.3836	1.0	2	5295.2587	0.5	8	4366.2700	0.6	5	4314.1576	0.7	9
4	2	3	7434.7912	0.2	5				5289.6641	0.6	6	4361.4804	0.5	7	4309.2303	0.8	7
4	3	1	7503.0507	1.0	6	5619.9408	0.7	3	5371.1831	0.7	6	4472.1173	0.2	4	4398.8585	0.6	9
4	3	2	7502.7533	0.6	6	5619.7692	0.4	2	5370.9452	0.5	5	4471.9642	0.8	4	4398.6734	0.9	6
4	4	0	7594.5943	1.0	3	5723.2047		1	5480.9008	0.6	3	4622.7618	1.2	3	4516.9900	0.7	3
4	4	1	7594.5948	0.5	4	5723.2067		1	5480.8997	0.3	3	4622.7613	1.0	4	4516.9878	1.2	3
5	0	5	7444.8787	0.3	4	5548.2706	0.1	2	5289.9540	0.7	7	4342.6147	0.9	6	4299.0304	0.7	3
5	1	4	7488.3767	0.5	4	5589.4986	0.6	2	5337.1403	0.6	8	4394.9058	0.1	4	4348.9915	0.4	3
5	1	5	7447.3616	0.9	3	5552.1896	0.6	3	5293.6824	0.8	10	4349.1460	0.3	5	4304.7896	0.4	5
5	2	3	7522.4570	0.5	4	5626.9458	1.1	4	5377.5171	0.4	5	4448.7313	0.2	5	4395.0853	0.5	6
5	2	4	7509.8514	0.5	5	5617.3145	0.7	5	5365.5223	0.6	7	4438.2082	1.0	6	4384.3897	0.7	7
5	3	2	7580.9649	0.6	5	5695.2570	0.6	3	5449.5876	0.5	9	4551.0368	0.2	5	4476.0037	0.4	8
5	3	3	7579.8115	0.9	7	5694.5846		1	5448.6595	0.7	9	4550.4323	0.2	5	4475.2823	0.3	8
5	4	1	7671.4495	0.6	5	5797.8109		1	5558.3597	0.8	7	4700.9903	0.6	4	4593.2523	0.4	5
5	4	2	7671.4191	0.5	7				5558.3389	0.7	6	4700.9795	0.4	4	4593.2377	0.6	6
5	5	0	7788.1610	0.8	2	5930.0345	1.8	2	5697.3013	0.6	3				4741.2479	0.8	3
5	5	1	7788.1589	0.3	3	5930.0351		1	5697.3009	0.4	4				4741.2481	0.7	4
6	0	6	7526.3535	0.9	2	5629.2814	0.9	2	5372.4003	0.4	10	4426.2444	0.6	5	4381.5609	0.4	3
6	1	5	7583.3106	0.9	6	5682.7213	0.6	3	5433.8549	0.9	9	4493.5496	1.0	5	4445.5929	0.6	4
6	1	6	7527.6770	0.4	7	5631.6038	0.2	3	5374.5303	0.5	8	4430.4204	0.2	4	4385.1105	0.9	5
6	2	4	7621.2403	0.8	6	5722.1584	0.9	2	5477.2171	0.6	8	4548.9668	0.5	6	4493.2736	0.4	5
6	2	5	7599.0856	0.5	5	5704.7525	0.6	4	5455.7725	0.7	11	4529.6233	0.4	7	4473.8875	0.7	7
6	3	3	7675.5403	0.7	8	5786.3555		1	5544.6087	0.4	6	4646.4204	0.8	4	4569.3534	0.3	7
6	3	4	7672.2697	0.2	5	5784.4114	1.4	2	5541.9435	0.4	8	4644.6622	0.6	5	4567.2640	0.4	8
6	4	2	7763.9643	0.6	4				5651.5549	0.9	7	4795.0290	0.5	5	4684.9712	0.3	3
6	4	3	7763.8127	0.6	7				5651.4477	0.5	7	4794.9750	0.4	5	4684.8970	0.4	3
6	5	1	7880.0637	0.8	2				5789.9176	0.9	4				4832.3919	0.4	3
6	5	2	7880.0643	0.1	3				5789.9179	0.5	3				4832.3924	0.2	4
6	6	0	8020.9517		1				5956.5304	0.4	3				5009.2343	0.1	3
6	6	1	8020.9494	1.0	4				5956.5299	1.0	3				5009.2343	0.2	3
7	0	7	7619.9225	0.6	5	5722.2772	0.2	2	5466.9039	0.5	7	4521.9294	0.5	5	4475.9838	0.9	3
7	1	6	7691.4392	0.1	2	5789.5644	1.2	3	5544.2587	0.6	8	4606.7313	0.8	3	4556.0881	0.7	6
7	1	7	7620.5940	1.0	3	5723.5830	0.6	3	5468.0606	0.2	4	4524.4786	0.2	4	4478.0671	0.5	5
7	2	5	7736.4991	0.4	4	5833.6951	0.2	2	5593.8679	0.7	7	4666.7652	0.2	3	4608.3747	0.3	6
7	2	6	7702.1022	0.4	6	5805.9411	0.4	2	5560.0391	0.2	7	4635.3939	0.6	3	4577.3834	0.5	6
7	3	4	7787.4046	0.5	5	5893.7360	0.0	2	5656.8531	0.8	7	4758.7571	0.1	4	4679.4380	0.8	5
7	3	5	7779.9240	0.3	8	5889.1302	0.4	3	5650.6370	0.8	6	4754.5552	0.6	5	4674.5002	0.6	6
7	4	3	7872.3677	0.9	7				5760.6655	0.3	3	4904.9863	0.6	4	4792.2887	0.4	6
7	4	4	7871.8266	0.7	7				5760.2855	0.2	7	4904.7964	0.9	5	4792.0231	0.6	4
7	5	2	7987.4607		1				5898.1179	1.0	4				4938.8468	1.1	3

Note. N is the number of lines used for the upper level determination and δ denotes the experimental uncertainties (combination differences) in 10^{-3} cm^{-1}.

(*continued on next page*)

Table 7 (*continued*)

			(002)			(200)			(011)			(030)			(110)		
J	K_a	K_c	E	δ	N	E	δ	N	E	δ	N	E	δ	N	E	δ	N
	1		2	3	4	5	6	7	8	9	10	11	12	13	14	15	16
7	5	3	7987.4466	0.7	2				5898.1060	0.5	2				4938.8435	1.2	5
7	6	1	8127.7872	1.0	3				6064.1724	0.3	4				5114.4963	0.9	2
7	6	2	8127.7875	1.0	3				6064.1720	0.5	4				5114.4973		1
7	7	0	8291.9131	0.9	2				6257.0593		1						
7	7	1	8291.9131	0.9	2				6257.0593		1						
8	0	8	7725.6519	0.5	5	5827.2789	0.1	2	5573.5157	0.5	4	4629.6390	0.5	2	4582.3191		1
8	1	7	7811.8601	1.0	4	5909.1773	0.7	3	5667.3594	0.5	7	4733.5278	0.8	4	4679.4913	0.6	5
8	1	8	7725.9819	0.8	4	5827.9865	0.6	2	5574.1238	0.7	4	4631.1448	0.5	2	4583.5001	0.2	3
8	2	6	7867.3641	0.6	6	5960.9826	0.2	2	5726.7089	0.8	5	4801.6134	1.2	4	4739.7526	0.7	5
8	2	7	7818.5091	0.6	4	5920.5561	0.9	3	5677.9342	0.4	5	4755.1684	0.1	3	4694.5187	0.6	4
8	3	5	7916.9470	0.9	6	6017.8519		1	5786.8338	0.4	5	4888.5817	0.8	4	4806.7791	0.6	5
8	3	6	7902.4632	0.9	6	6008.5527		1	5774.4782	0.6	8	4879.9308	0.5	3	4796.7748	0.4	6
8	4	4	7997.0064	1.0	4				5885.9614	0.9	4	5031.0246	0.6	3	4915.4166	0.4	5
8	4	5	7995.4568	0.9	4				5884.8666	0.8	5	5030.4682	1.0	3	4914.6444	1.0	6
8	5	3	8110.4411	1.0	4				6021.9689	0.8	4				5060.6731	0.9	4
8	5	4	8110.3722	0.6	5				6021.9248	0.5	3				5060.6471	0.4	4
8	6	2	8250.0046	1.0	3				6187.2765	1.0	2						
8	6	3	8250.0024	0.4	3				6187.2751	0.4	2						
8	7	1	8413.5291	0.3	3												
8	7	2	8413.5291	0.4	3												
8	8	0							6598.0065		1						
8	8	1							6598.0065		1						
9	0	9	7843.5895	0.7	3	5944.3315	1.4	2	5692.2957	0.3	4	4749.4123	1.0	3	4700.6351	1.4	2
9	1	8	7944.0807	0.6	5	6040.8649	0.9	3	5802.4531	0.6	3	4873.0725	0.6	2	4814.9792	0.7	5
9	1	9	7843.7469	0.1	2	5944.7077	0.7	3	5692.6074	0.2	4	4750.2821	0.6	3	4701.2868	1.1	2
9	2	7	8012.7785	1.0	5	6103.2614		1	5874.7945	0.6	4	4952.7690	0.4	3	4886.5843	0.1	2
9	2	8	7947.9517	0.9	4	6048.2800	0.1	2	5809.0919	0.8	5	4888.5951	0.8	5	4824.9438	0.7	4
9	3	6	8064.0610	0.4	5				5934.7031	0.5	4	5036.3236	1.0	3	4951.6630	0.5	5
9	3	7	8039.4970	0.1	4	6142.4117	1.3	2	5913.1203	0.8	8	5020.5274	0.4	2	4933.8181	0.2	4
9	4	5	8138.3699	1.0	5				6027.8433	0.8	2				5054.6645	1.0	4
9	4	6	8134.6165	0.6	2				6025.1429	1.0	4				5052.7421	0.4	3
9	5	4	8249.1350	1.0	3				6161.5615		1				5197.9393	0.7	3
9	5	5	8248.9021	1.0	2				6161.4210	1.0	3				5197.8495	1.0	4
9	6	3	8387.6351	2.0	5				6325.8772	1.0	2						
9	6	4	8387.6348	0.7	3				6325.8770	2.0	2						
9	7	2	8550.4131		1												
9	7	3	8550.4130	0.6	2												
10	0	10	7973.7559		1	6073.4724	1.0	2	5823.2816	0.3	4	4881.2947	0.4	2	4830.9901	1.0	2
10	1	9	8087.9937	1.0	3				5949.2381	0.7	4	5024.7181	0.1	2	4962.0782	0.2	3
10	1	10	7973.8246	1.0	2	6073.6663	1.1	2	5823.4390	0.7	4	4881.7875	0.3	2	4831.3464	0.1	2
10	2	8	8171.5725	0.7	4	6259.6662		1	6037.0318	0.7	4				5047.9061	0.5	2
10	2	9	8090.1325	0.9	3	6188.8287	0.1	2	5953.1947	1.0	3	5035.3390	0.8	2	4968.3399	0.4	2
10	3	7	8228.1329	0.7	4				6100.1140	0.9	3				5113.9830	0.9	3
10	3	8	8190.5855	0.8	4	6290.3821	0.4	2	6066.1520	1.0	7				5085.2669	0.0	2
10	4	6	8297.0338	0.1	2				6186.8042	0.7	4				5210.4457	0.5	2
10	4	7	8289.1108	0.4	2				6180.9713	0.4	2				5206.2379	0.7	2
10	5	5	8403.7337	0.5	2				6317.0324		1						
10	5	6	8403.0557	0.6	2				6316.6074		1						
11	0	11	8116.1438		1	6214.7075	0.7	2	5966.4812	0.7	3	5025.3076		1	4973.4169		1
11	1	10	8243.6849		1	6339.2429	0.7	2	6107.7076	0.5	3						
11	1	11	8116.1768	1.0	2	6214.8009		1	5966.5590	0.4	3	5025.5859		1	4973.6084		1
11	2	9	8342.6533	1.0	4	6429.2249		1	6212.2719	1.0	4				5222.6605		1
11	2	10	8244.8156	1.0	3	6341.9657		1	6109.9697		1						
11	3	8	8408.2080	1.0	2												
11	3	9	8355.2737	0.7	3				6233.1484	1.0	3						
11	4	7	8473.4480	0.6	3				6363.3639	0.4	2						
11	4	8	8458.6422		1												
11	5	6	8574.5072	0.8	2												
11	5	7	8572.8234		1												
12	0	12	8270.7376	2.0	2	6368.0121		1	6121.8881	1.0	3	5181.4624		1	5127.9330		1
12	1	11	8603.1511		1	6505.8927		1	6277.9665	0.9	2						
12	1	12	8270.7463		1	6368.0616		1	6121.9236		1	5181.6186		1	5128.0350		1
12	2	10	8525.2800		1												

Table 7 (*continued*)

			(002)			(200)			(011)			(030)			(110)		
J	K_a	K_c	E	δ	N	E	δ	N	E	δ	N	E	δ	N	E	δ	N
	1		2	3	4	5	6	7	8	9	10	11	12	13	14	15	16
12	2	11	8411.8558		1				6279.2231	0.2	2						
12	3	9							6480.2985		1						
12	3	10	8533.1325		1				6413.6522		1						
12	4	8	8667.6481	1.0	2												
12	5	7	8761.8774		1												
12	5	8	8758.0914		1												
13	0	13													5294.5312		1
13	1	12				6684.3004		1									
13	1	13				6533.3922		1	6289.4987		1				5294.5741		1
13	2	11				6804.3172		1	6598.2236		2						
13	2	12	8591.1225		1				6460.8070	1.0	2						
13	3	10							6460.1230	1.0	1						
14	0	14	8616.4177		1				6469.2261		1				5473.1957		1
14	1	14	8616.4177		1												

Table 8
Spectroscopic parameters of the (000), (010), (020), (100), (001), (011), (200), and (002) vibrational states of $HD^{18}O$ (in cm^{-1})

	(000)	(010)	(020)	(100)	(001)	(011)	(200)	(002)
E	0	1396.26715(40)	2767.2030(21)	2709.2929(14)	3696.33022(36)	5071.49629(47)	5335.36189(98)	7229.18576(58)
A	23.110310(27)	25.16599(14)	27.63242(97)	23.02060(74)	22.08749(11)	23.97815(22)	22.6320(13)	21.09042(30)
B	9.059135(12)	9.192757(34)	9.30825(19)	8.89735(17)	9.049520(40)	9.189927(63)	8.70728(22)	9.039264(69)
C	6.360901(12)	6.278102(26)	6.20879(20)	6.24851(10)	6.283315(31)	6.199903(40)	6.14933(15)	6.205176(61)
$\Delta_K \times 10^2$	1.18744(38)	2.2309(12)	3.059(13)	2.534(12)	1.0845(11)	2.0654(26)	1.780(49)	0.9039(69)
$\Delta_{JK} \times 10^3$	1.2734(11)	1.1136(46)	0.489(23)	1.814(22)	1.1041(34)	0.9654(77)	2.238(26)	0.9322(67)
$\Delta_J \times 10^3$	0.35318(13)	0.40399(45)	0.4322(24)	3.774(15)	0.38582(40)	0.41599(69)	3.334(22)	0.3739(10)
$\delta_K \times 10^3$	2.0836(53)	3.4569(56)	4.390(62)	3.298(20)	1.9523(51)	3.329(12)	3.353(61)	1.8581(56)
$\delta_J \times 10^3$	0.118001(89)	0.14414(16)	0.15924(65)	0.13329(97)	0.12464(25)	0.15106(47)	0.1079(14)	0.13056(42)
$H_K \times 10^4$	0.4575(20)	1.2029(45)	0.070	6.996(77)	0.3858(40)	1.379(12)	2.42(67)	0.372(29)
$H_{KJ} \times 10^5$	−0.863(18)	−1.732(28)	−4.33(19)	0.142	−0.720(25)	−1.854(62)	—	−0.988(30)
$H_{JK} \times 10^6$	2.359(63)	4.707(74)	6.82(57)	5.46(17)	1.966(91)	5.90(20)	15.93(57)	2.833(90)
$H_J \times 10^6$	0.03708(83)	0.0556(15)	0.025	0.1154(73)	0.0437(15)	0.0407(39)	−0.0708	0.0260(94)
$h_K \times 10^5$	1.477(81)	4.447(62)	5.50(48)	6.87(29)	1.141(65)	4.63(24)	11.44(50)	1.603(96)
$h_{JK} \times 10^6$	1.069(39)	1.643(55)	1.08(35)	2.78(13)	0.906(52)	1.75(10)	1.82(33)	1.037(65)
$h_J \times 10^6$	1.658(50)	0.02677(53)	—	0.0658(39)	0.0208(12)	0.0224(23)	−0.00368	0.0198(18)
$L_K \times 10^6$	−0.174(11)	−0.6722(99)	−0.376(87)	−16.30(19)	−0.1609(78)	−1.354(42)	—	−0.210(75)
$L_{KKJ} \times 10^7$	0.187	1.71(11)	—	—	0.791(95)	1.16(49)	19.1(17)	0.907
$L_{KJ} \times 10^7$	−0.0293	−0.514(44)	—	−2.41(33)	−0.324(34)	−0.419	−3.84(21)	−0.221(90)
$L_{KJJ} \times 10^9$	−0.681	−1.92(31)	—	—	2.25(41)	−4.00	—	−3.81(34)
$l_K \times 10^6$	−0.0324	−0.320(27)	—	−1.14(13)	−0.114(14)	−0.261(84)	—	−0.153(39)
$l_{KJ} \times 10^8$	−0.398	−1.39(26)	—	—	2.22(28)	−1.86(80)	—	—
$l_{JK} \times 10^9$	−0.134	−0.734	—	—	−0.720	—	—	—
$P_K \times 10^7$	0.00456(20)	0.0131(11)	—	−1.610(16)	0.00224(26)	0.0923(16)	−0.358	0.00696
$p_K \times 10^9$	0.0126	−0.549	—	14.0(12)	0.052	—	—	—
$\sigma \times 10^3$	0.194	1.06	4.97	3.32	0.924	1.09	1.82	1.33

Acknowledgments

The authors are indebted to O. Naumenko of IAO (Russia) for suggestions and discussions. This work was jointly supported by the Natural Science Foundation of China (20473079 and 10574124), and by the Chinese Academy of Sciences.

Appendix A. Supplementary data

Supplementary data for this article are available on ScienceDirect (www.sciencedirect.com) and as part of the Ohio State University Molecular Spectroscopy Archives (http://msa.lib.ohio-state.edu/jmsa_hp.htm).

References

[1] G. Steenbeckeliers, J. Bellet, Compt. Rend. 273B (1971) 471–474.
[2] F.X. Powell, D.R. Johnson, Phys. Rev. Lett. 24 (1970) 647.
[3] F.C. De Lucia, P. Helminger, R.L. Cook, W. Gordy, Phys. Rev. Lett. A6 (1972) 1324–1326.
[4] P. Helminger, F.C. De Lucia, J. Mol. Spectrosc. 70 (1978) 263–269.
[5] F.C. De Lucia, P. Helminger, W.H. Kirchhoff, J. Phys. Chem. Ref. Data 3 (1974) 211–219.

[6] F. Winther, J. Mol. Spectrosc. 65 (1977) 405–419.
[7] R.A. Toth, J.-M. Flaud, C. Camy-Peyret, J. Mol. Spectrosc. 67 (1977) 206–218.
[8] R.A. Toth, J.-M. Flaud, C. Camy-Peyret, J. Mol. Spectrosc. 67 (1977) 185–205.
[9] P. Helminger, J. Mol. Spectrosc. 70 (1978) 263–269.
[10] C. Camy-Peyret, J.-M. Flaud, N. Papineau, CR. Acad. Sci. B Phys. 290 (1980) 537–540.
[11] C. Camy-Peyret, J.-M. Flaud, R.A. Toth, J. Mol. Spectrosc. 87 (1981) 233–241.
[12] J.-P. Chevillard, J.-Y. Mandin, J.-M. Flaud, C. Camy-Peyret, Can. J. Phys. 63 (1985) 1112–1127.
[13] A.D. Bykov, V.N. Saveliev, O.N. Ulenikov, J. Mol. Spectrosc. 118 (1986) 31–315.
[14] J.-P. Chevillard, J.-Y. Mandin, C. Camy-Peyret, J.-M. Flaud, Can. J. Phys. 64 (1986) 746–761.
[15] J.-P. Chevillard, J.-Y. Mandin, J.-M. Flaud, C. Camy-Peyret, Can. J. Phys. 65 (1987) 777–789.
[16] O.N. Ulenikov, A.S. Zhilyakov, J. Mol. Spectrosc. 133 (1989) 239–243.
[17] R.A. Toth, J. Opt. Soc. Am. B 9 (1992) 462–482.
[18] R.A. Toth, J. Opt. Soc. Am. B 10 (1993) 1526–1544.
[19] R.A. Toth, J. Mol. Spectrosc. 166 (1994) 184–203.
[20] R.A. Toth, Appl. Opt. 33 (1994) 4869.
[21] A. Bykov, O. Naumenko, T. Petrova, A. Scherbakov, L. Sinitsa, J.-Y. Mandin, C. Camy-Peyret, J.-M. Flaud, J. Mol. Spectrosc. 172 (1995) 243–253.
[22] R.A. Toth, J. Mol. Spectrosc. 190 (1998) 379–396.
[23] M. Tanaka, J.-W. Brault, J. Tennyson, J. Mol. Spectrosc. 216 (2002) 77–80.
[24] M. Tanaka, O. Naumenko, J.W. Brault, J. Tennyson, J. Mol. Spectrosc. 234 (2005) 1–9.
[25] M. Tanaka, M. Sneep, W. Ubachs, J. Tennyson, J. Mol. Spectrosc. 226 (2004) 1–6.
[26] P. Macko, D. Romanini, S.N. Mikhailenko, O.V. Naumenko, S. Kassi, A. Jenouvrier, Vl.G. Tyuterev, A. Campargue, J. Mol. Spectrosc. 227 (2004) 90–108.
[27] A.-W. Liu, O. Naumenko, K.-F. Song, B. Voronin, S.-M. Hu, J. Mol. Spectrosc. 236 (2006) 127–133.
[28] A.-W. Liu, S.-M. Hu, C. Camy-Peyret, J.-Y. Mandin, O. Naumenko, B. Voronin, J. Mol. Spectrosc. 2006, in press.
[29] L.S. Rothman, D. Jacquemart, A. Barbe, D. Chris Benner, M. Birk, L.R. Brown, M.R. Carleer, C. Chackerian Jr., K. Chance, L.H. Coudert, V. Dana, V.M. Devi, J.-M. Flaud, R.R. Gamache, A. Goldman, J.-M. Hartmann, K.W. Jucks, A.G. Maki, J.-Y. Mandin, S.T. Massie, J. Orphal, A. Perrin, C.P. Rinsland, M.A.H. Smith, J. Tennyson, R.N. Tolchenov, R.A. Toth, J. Vander Auwera, P. Varanasi, G. Wagner, J. Quant. Spectrosc. Radiat. Transf. 96 (2005) 139–204.
[30] H. Partridge, D.W. Schwenke, J. Chem. Phys. 106 (1997) 4618–4639.
[31] D.W. Schwenke, H. Partridge, J. Chem. Phys. 113 (2000) 6592–6597.
[32] R.A. Roth, J. Mol. Spectrosc. 162 (1993) 20–40.
[33] W.F. Wang, T.L. Tan, B.L. Tan, P.P. Ong, J. Mol. Spectrosc. 176 (1996) 226–228.
[34] R.A. Toth, J. Mol. Struc. 742 (2005) 49–68.
[35] J.K.G. Watson, J. Chem. Phys. 46 (1967) 1935–1949.
[36] O.N. Ulenikov, G.A. Onopenko, I.M. Olekhnovitch, S. Alanko, V.-M. Horneman, M. Koivusaari, R. Anttila, J. Mol. Spectr. 189 (1998) 74–82.